Proposal of Reducing Impact Force Control System for Scan Stage with Decouplable Structure of Coarse and Fine Parts

Kyota Tokuyama and Hiroshi Fujimoto
The University of Tokyo
Tokyo, Japan
Email: tokuyama@hflab.k.u-tokyo.ac.jp
fujimoto@k.u-tokyo.ac.jp

Daisuke Yumiza and Kazuaki Saiki
Nikon Corporation
Yokohama, Japan
Email: Yumiza.Daisuke@nikonoa.net
saiki.kazu@nikon.co.jp

***Abstract*—The upsizing and obtaining higher control accuracy are required for many large industrial machines. However, the requirements are trade-off against each other from the viewpoint of the conventional machine structure. In this paper, a novel structure of stage consists of coarse driving part and fine driving part, which can be uncoupled with each other, is examined. In this case, the fine part can be simplified so that it would be more rigid and has higher resonant frequencies. One problem of the structure is that the impact between the fine part and the coarse part happens at the beginning of the acceleration/deceleration. Therefore, we also design an practical control approach for reducing the impact force to improve the control performance. We also discuss on designing a control system for reducing the impact force between the coarse part and the fine part. The effectiveness of the proposed approach is verified via simulations and experiments.**

I. Introduction

Demands of large liquid crystal display (LCD) and mobile tools are increasing, and their upsizing, higher resolution, and improvement of production rate are required. Therefore, higher speed and higher precision of industrial machine, such as the embedded stages, become necessary. These stages may have a structure consists of coarse and fine part for follow-up high-speed and high-precision control [1][2]. In this case, the structure of the fine part can be simplified and the weight can be reduced. As a result, resonant frequencies of the fine part can be improved as well as the bandwidth of the feedback control loop [3]. Some similar structures are also studied in assembly robot [4], HDD [5], optical disk [6], etc.

In general, coarse part and fine part are controlled independently. Control law is simple, but the fine part also needs a motor to generate thrust for acceleration and deceleration.. For instance, in the case of HDD controlled by dual actuators, the fine part is positioning while the coarse part is stop. Thus, disturbance at the coarse part does not affect on the fine part. However, in the case of scan stages, the coarse and fine parts need to move together. Therefore, disturbance at the coarse part would affect the fine part. As the fabrication is performed when stages move at the constant speed, we consider to decouple the coarse and fine parts during the constant speed and couple them in the acceleration and deceleration. In this case, the weight of the fine stage can be reduced, which is advantageous for high-speed and high-accuracy control. Motivated by this idea, we present a novel stage with decouplable structure of coarse and fine part, as shown in Fig. 1.

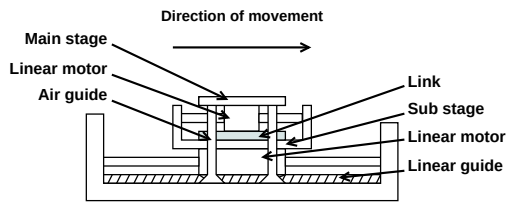

(a) 2D model.

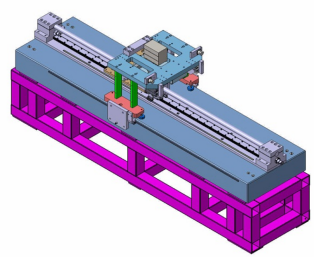

(b) 3D model.

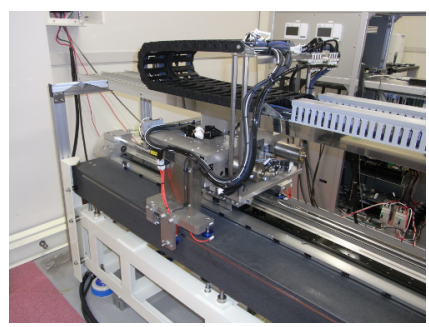

(c) Real machine.

Fig. 1. Catapult stage.

In this paper, for convenience, the stage is called as 'catapult stage', and the coarse part and the fine part are referred to 'sub

TABLE I
CATAPULT STAGE PARAMETERS.

Maximum thrust force of main stage F_{mm}	80.0	N
Maximum thrust force of sub stage F_{sm}	327	N
Mass of main stage m	14.4	kg
Mass of sub stage M	37.5	kg
Coefficient of viscosity of sub stage D	129	N · s/m

stage' and 'main stage', respectively. We use high power thrust motor for sub stage to accelerate and decelerate the stage. On the other hand, we use small power motor for main stage to obtain high-precision positioning.

As the stage is divided into coarse and fine part, the degree of freedom of stage design is expanded, and more freedom is given for controller design. As a result, higher speed and more precisely positioning will be possible.

Due to the inherent impact between the main stage and sub stage, the control performance would be deteriorated. Hence, the impact force must be reduced when the table is accelerated and decelerated by the sub stage. In our prior work, we modeled the impact force at the link and reduce the impact force by feedforward control [7]. However, the modeling error is unavoidable and the impact force cannot be removed completely. In this paper, we propose reducing impact force control by introducing virtual spring and virtual damper to the link.

The remainder of this paper is organized as follows. Section II presents structure of the catapult stage and modeling of the stage. Section III proposes impact force reducing control method of the catapult stage. Section IV shows the comparison of conventional method and proposed method by simulation and experiment. Finally, conclusion is given in Section V.

II. MODELING OF THE CATAPULT STAGE

A. Structure of the stage

The main stage and the sub stage are driven by linear motors. In the main stage, air guide is used, and therefore viscous term can be ignored. In the sub stage, oil–lubricated linear guide is used and the viscous coefficient is denoted by D. The transfer function of the main stage P_m and the sub stage P_s are expressed as follows.

$$P_m = \frac{1}{ms^2} \tag{1}$$

$$P_s = \frac{1}{Ms^2 + Ds} \tag{2}$$

The parameters of the stage are shown in Table I.

Top view of the link between the main stage and the sub stage is shown in Fig. 2. In addition, we show each parameter of the link in Table II. Oval piece is assembled through stepping motor in the main stage. Thus, the direction of the oval piece can be switched between the major axis direction and the minor axis direction. Square frame and load cell are

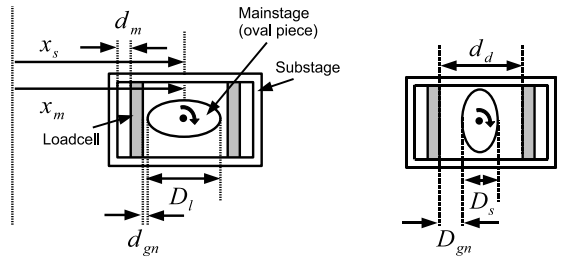

(a) Link (before rotate). (b) Link (after rotate).

Fig. 2. Link.

TABLE II
LINK PARAMETERS.

Stiffness of load cell K_r	375	N/mm
Maximum displacement of load cell d_m	2.00×10^{-4}	mm
Diameter of long axis of oval piece D_l	68.0	mm
Diameter of short axis of oval piece D_s	58.0	mm
Gap(Mode a) d_{gn}	0.5	mm
Gap(Mode c) D_{gn}	5.5	mm
Distance of load cell d_d	69.0	mm

assembled in the sub stage as shown in Fig. 2. Thus, the main stage can be moved by sub stage via the load cell and the oval piece. As shown in Fig. 3, when major axis direction of the oval piece faces the direction of movement and there is no contact between the oval piece and the load cell, the mode is denoted by Mode a. When there is contact between the left part of the oval piece and the load cell, the mode is denoted by Mode b. When there is contact between the right part of the oval piece and the load cell, the mode is denoted by Mode c. When minor axis direction of the oval piece faces direction of movement, the mode is denoted by Mode d.

In the case of Mode a, there is gap d_{gn} between the oval piece and the load cell. In the Mode c, there is gap D_{gn}. Thus, in the case of Mode c, if we can control the gap between the center position of the main stage and the sub stage to be less than 5.5 mm, the main stage and the sub stage can be decoupled.

B. Modeling

As shown in Fig. 4, catapult stage can be viewed as a two–inertia system consists of the main stage and the sub stage. x_m, x_s are the absolute positions of the main stage and the sub stage, F_m, F_s are the input thrust of the main stage and the sub stage, LINK is the block of the link, F_L denotes the force occurred at the link. LINK has impact force F_i, elastic force by the load cell F_r.

$$F_L = F_i + F_r. \tag{3}$$

1) Modeling for impact force [8]: When the main stage hits the sub stage, the impact force F_i occurs between the flat surface A and hemisphere B. An example is shown in Fig. 5. By Hertz contact theory, the impact force F_i is given by

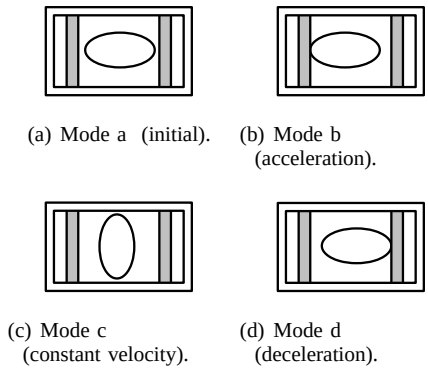

(a) Mode a (initial). (b) Mode b (acceleration).

(c) Mode c (constant velocity). (d) Mode d (deceleration).

Fig. 3. Link model of each mode.

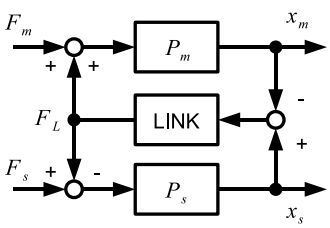

Fig. 4. Block diagram of catapult stage.

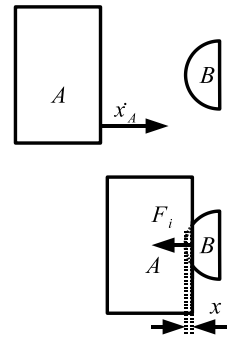

Fig. 5. Model of impact force.

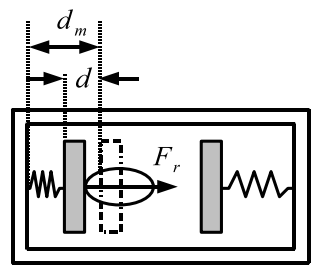

Fig. 6. Model of link w/o impact force.

$$F_i = -Kx^{3/2} - \alpha|x|^{1/2}\dot{x}, \tag{4}$$

where K is non–linear spring coefficient and α is non–linear damper coefficient.

2) Modeling for load cell: We consider the force that occurs when load cell deforms elastically. As shown in Fig. 6, the load cell can be considered as a linear spring. Thus, when the load cell has displacement d, Fr can be expressed by

$$F_r = \begin{cases} K_r d & (|d| < d_m) \\ K_r d_m & (|d| \geq d_m). \end{cases} \tag{5}$$

3) Modeling for the LINK: We add dead zone to the model derived in Section II-B1, II-B2 to estimate gap between the main stage and the sub stage. Moreover we formulated LINK model, as shown in Fig. 7.

Additionally, we measure the force occurred at the link and identify the parameters K, α and the width of the dead zone of the LINK. We estimate the force F_L occurred at the link when the sub stage is moved along with the reference velocity, as shown in Fig. 8. We can estimate the force occurred at the link from (6), (7) by disturbance observer (DOB) from input thrust of the sub stage F_s and position of the sub stage x_s.

$$x_s = \frac{1}{Ms^2 + Ds}(F_s - F_L) \tag{6}$$

Thus,

$$\hat{F}_L = F_s - (M\ddot{x}_s + D\dot{x}_s). \tag{7}$$

where $\hat{F}_L$ is estimation value of the force occurred at the link F_L.

In Fig. 9, the solid line shows the output of DOB and the dotted line shows the estimated force. The parameters of the LINK are tuned to let the solid line fit the dotted line.

4) Modes model: Catapult stage model is shown in Fig. 10. Mode a, b, c, d are given by switching SW1, SW2. Block diagram of each Mode is shown in Fig. 11. Mode a is shown in Fig. 11(a) that SW1 and SW2 in Fig. 10 are off. Mode b, d are shown in Fig. 11(b) that SW1 and SW2 in Fig. 10 are off and on respectively. Moreover, Mode c is Fig. 11(c) that SW1 and SW2 in Fig. 10 are on and off respectively.

III. Control method of catapult stage

First, before moving, the load cell should be controlled to touch the oval piece so that the thrust propagated from the sub stage to the main stage can be soft. In order to do this, the main stage is stopped and the sub stage is control to follow a step command.

Next, we control the sub stage to follow a position reference by integrating the velocity which is shown in Fig. 8. The control of the main stage is start when the reference shifts from acceleration to constant speed. In the following, a novel control method is proposed to reduce the impact force.

A. Impact force reduction by feedforward control (conventional method)

The velocity signal shown in Fig. 12 is used instead of the signal shown in Fig. 8. The integrations of the velocity signals shown in Fig. 12 are used as the position reference. Note that the main stage is controlled only from 0.5 s to 1.5 s.

In Mode c, the position reference of the sub stage is reduced a little at 0.5 s to decouple the stages. Moreover, the position

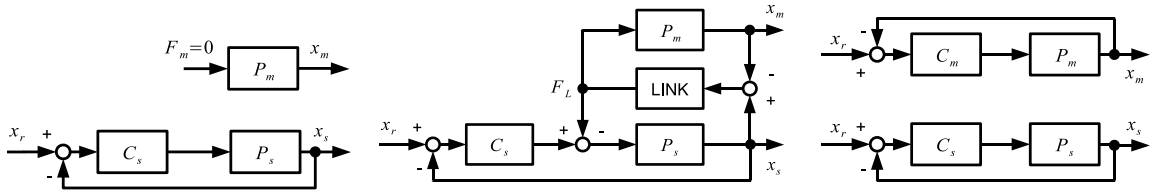

(a) Mode a (SW1=OFF, SW2=OFF). (b) Mode b, d (SW1=OFF, SW2=ON). (c) Mode c (SW1=ON, SW2=OFF).

Fig. 11. Block diagrams of each mode.

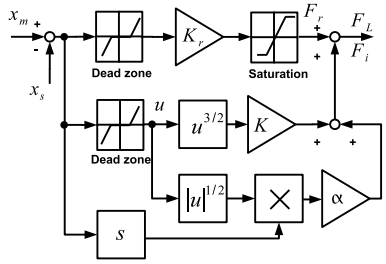

Fig. 7. Block diagram of link.

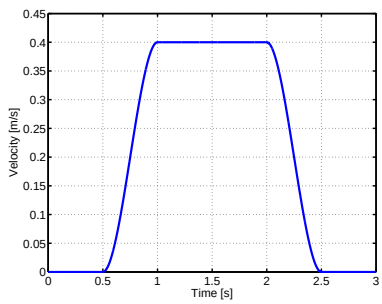

Fig. 8. Reference velocity signal.

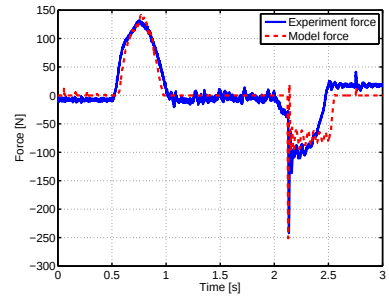

Fig. 9. Impact force in experiment.

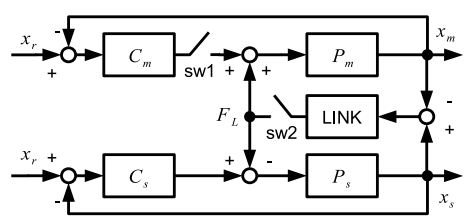

Fig. 10. Block diagram of simulation.

reference of the sub stage is reduced a little again at 1.4 s to reduce the impact force. The amplitude of the reduction is the gap between the oval piece and the load cell.

B. Virtual spring and virtual damper (proposed method)

We add feedback control to the conventional method explained in Section III-A. As shown in Fig. 13, we introduce virtual spring and virtual damper to reduce the impact force that work when relative position is negative. In this figure, K_V, D_V are virtual spring coefficient and virtual damper coefficient. These parameters are shown in Table III.

Proposed block diagram is shown in Fig. 14, where the P–PI controller is used as the compensator, and P_{sn} is nominal model of the sub stage. P_{sn} generates additional position signal.

In this figure, V is expressed as the transfer function:

$$V = K_V + D_V s \tag{8}$$

1) Stability of proposed method: We analyze the stability of the control system shown in Fig. 14. Loop transfer function L_s from the reference position of the sub stage x_{sr} to the position of the substage x_s and loop transfer function L_m from the position of the main stage x_m to the position of the substage x_s are shown as follows.

$$L_s = \frac{P_s C_{sv} C_{sp}}{1 + P_s V + s P_s C_{sv} + P_s P_{sn} C_{sv} C_{sp} V} \tag{9}$$

$$L_m = \frac{P_s V + P_s P_{sn} C_{sv} C_{sp} V}{1 + s P_s C_{sv} + P_s C_{sv} C_{sp}} \tag{10}$$

Feedback controller is designed by pole placement method. The pole of velocity loop is -100 Hz and the pole of the position loop is -10 Hz. In this case, Bode diagrams of L_s, L_m are shown as Fig. 15 and gain margin and phase margin are shown in Table IV. From Table IV, we can know that the proposed method is stable.

IV. Simulation and Experiment

A. Simulation

In this section, we simulate control method shown in Section III by the catapult model formulated in Section II-B3. We compare conventional method and proposed method when the modeling error of the gap has no error, +5 % error and -5 % error. FB controller is designed by pole placement method to plant model. The pole of velocity loop is -100 Hz and the pole of the position loop is -10 Hz.

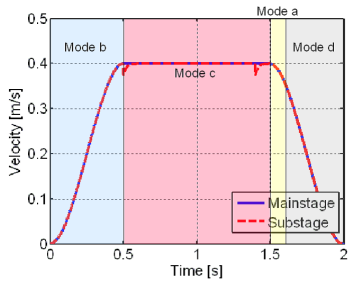

Fig. 12. Mode of link.

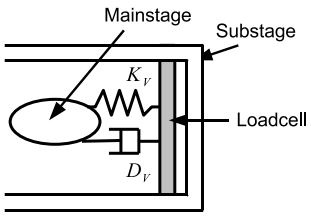

Fig. 13. Model of virtual spring and virtual damper.

The simulation results are shown in Fig. 16–18. The solid lines show the results of the conventional method, and the dotted lines show the results of the proposed method. From Fig. 16(d), we can know that maximum value of the force is larger but the settling time is not so changed. In addition, from Fig. 17(d) and Fig. 18(d), impact force is reduced when there is modeling error of the gap. From these results, we can confirm effectiveness of the proposed method.

B. Experiment

The experiments are also performed to verify the proposed method. In the following experiments, the main stage and the sub stage are controlled by velocity controller for the case of convenience. FB controllers are designed by pole placement method. The pole of velocity loop is -20 Hz. The experimental results are shown in Fig. 19. The solid lines show the results of the conventional method, and the dotted lines the results of the proposed method. Fig. 19(d) shows the comparison of the peek of the thrust of the sub stage in deceleration. It is observed that the impact force can be reduced by the proposed method.

V. Conclusion

In this paper, a novel structure of stage is presented for follow-up high-speed and high-precision control. However, due to the inherent impact between the main stage and sub stage, the control performance is deteriorated. In this paper, the impact force is reduced by introducing virtual spring and virtual damper. The proposed method can reduce the impact force even if the modeling error exists. The effectiveness of the proposed method is confirmed by simulation and experiment.

TABLE III
Virtual spring and virtual damper parameters.

Spring constant K_V	100	N/m
Damper constant D_V	3000	N·s/m

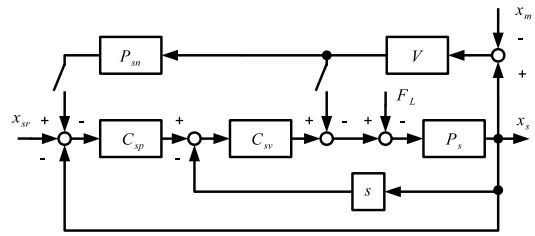

Fig. 14. Block diagram (proposed).

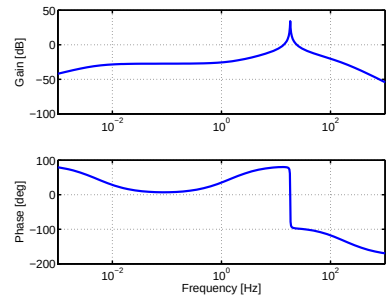

(a) L_s.

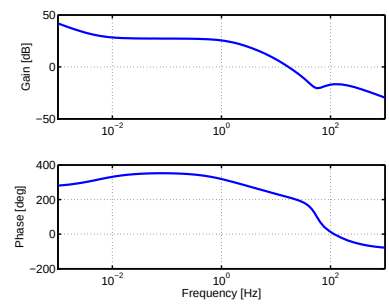

(b) L_m.

Fig. 15. Bode plot.

TABLE IV
Margin.

Gain margin of L_s	inf	dB
Gain margin of L_m	11.6	dB
Phase margin of L_s	82.2	deg
Phase margin of L_m	33.1	deg

References

[1] Norbert C. Cheung, Byron M. Y. Cheung, "Modelling and control of a high speed, long travel, dual voice coil actuator," in Proc. Int. Conf. Power Electronics and Drive Systems, Vol. 1, pp. 270–274, 1997

[2] Rong–Fong Fung, Yi–Lung Hsu, Ming–Shyan Huang, "System identification of a dual–stage XY precision positioning table," Precision Engineering, Vol. 33, No. 1, pp. 71–80, 2009

[3] Diederik Verscheure, Bart Paijmans, Hendrik Van Brussel, Jan Swevers, "Vibration and motion control design and trade–off for high–performance mechatronic systems," IEEE International Conference on Control Applications, pp. 1115–1120, 4–6 Oct. 2006

[4] Abdelhafid Omari, Aiguo Ming, Ghaylen Limam, Chisato Kanamori, Makoto Kajitani, Shuji Nakamura, "Development of a High Precision

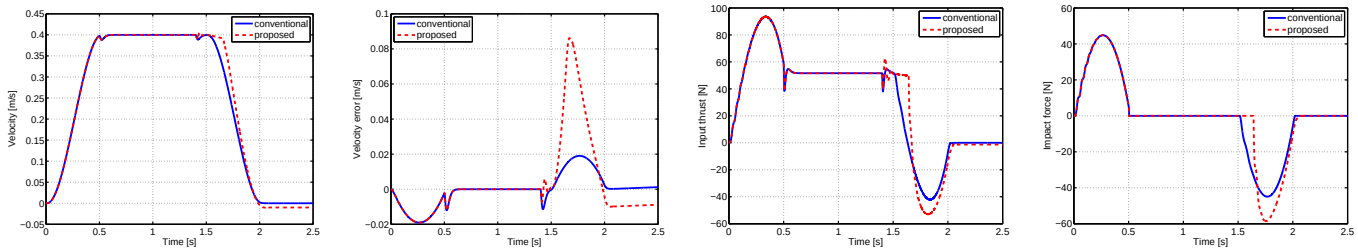

(a) Velocity. (b) Velocity error. (c) Input thurst. (d) Force from link.

Fig. 16. Simulation result w/o modeling error.

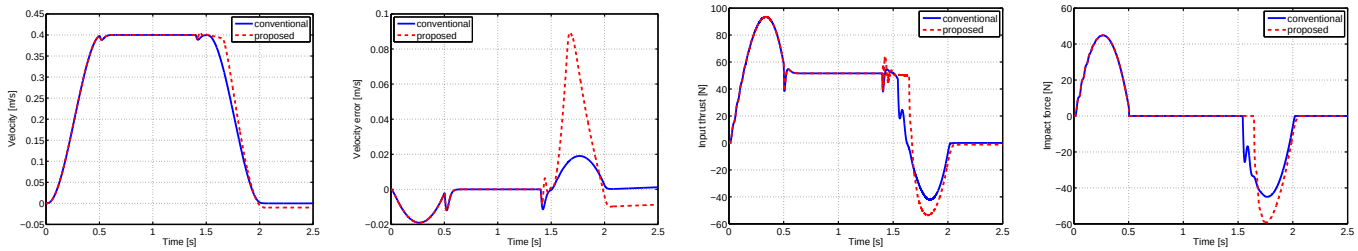

(a) Velocity. (b) Velocity error. (c) Input thurst. (d) Force from link.

Fig. 17. Simulation result w/ modeling error(+5%).

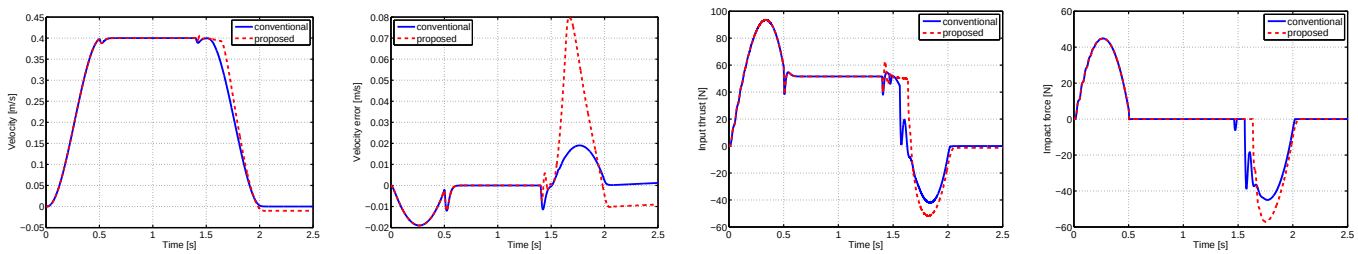

(a) Velocity. (b) Velocity error. (c) Input thurst. (d) Force from link.

Fig. 18. Simulation result w/ modeling error(-5%).

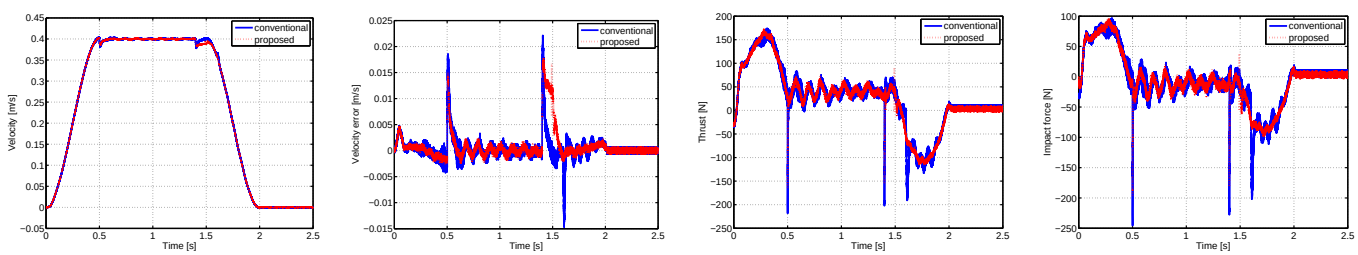

(a) Velocity. (b) Velocity error. (c) Input thurst. (d) Force from link.

Fig. 19. Experiment result.

Mounting Robot System With Fine Motion Mechanism (3rd Report)," Journal of the Japan Society for Precision Engineering, Vol. 67, No. 7, pp. 1101–1107, 2001

[5] Tetsuo Semba, Toshiki Hirano, John Hongt, Long–Sheng Fan, "Dual-Stage Servo Controller for HDD Using MEMS Microactuator," IEEE Trans. Magnetics, Vol. 35, No. 5, pp. 2271–2273, 1999

[6] Jian-Dong Yang, Xian-Deng Pei, "Seek time and trajectories of time optimal control for a dual stage optical disk drive actuator," IEEE Trans. Magnetics, Vol. 32, No. 5, pp. 3857–3859, 1996

[7] Kyota Tokuyama, Hiroshi Fujimoto, Daisuke Yumiza, Kazuaki Saiki, "Proposal of High–speed High–precision Control System for Stage with Decouplable Structure of Coarse and Fine Part," in Proc. of IIC2012, Vol. 2012, pp. 71–76, 2012(in Japnaese)

[8] Tetsuyuki Hongo, Hidenori Sato, Yoshio Iwata, Toshihiko Komatsuzaki, Yoko Hongo, "Modeling and Analysis of Impact System Composed of Ball and Plane," Transactions of the Japan Society of Mechanical Engineers Series C, Vol. 65, No. 634, pp. 2287–2293, 1999(in Japanese)